Tabriz Journal of Electrical Engineering (TJEE), vol. 55, no. 4, 2025 Serial no. 114
DOI: 10.22034/tjee.2025.66633.4995

Clamp-Conductor System Used for 63kV Overhead Power Lines: A Stress Analysis

J.Dadashizadeh Samakosh*

Department of Electrical and Computer Engineering, Babol Noshirvani University of Technology, Babol, Iran.

j.dadashizadeh@nit.ac.ir

*Corresponding author

Received: 07/04/2025, Revised: 19/08/2025, Accepted: 28/09/2025.

Abstract
A clamp-conductor system in power transmission lines serves two main functions: to withstand the conductor's tensile forces and to ensure reliable, continuous electrical current transfer. This study investigates the mechanical and thermal performance of a typical dead-end tension clamp-Lynx conductor system. A finite element model was developed to simulate the system's response to tensile and thermal stresses. The results indicate that the highest tensile stresses occur in the conductor's steel core and the clamp's steel anchor. Thermal performance was evaluated through both finite element simulation and laboratory current-injection testing. Findings show that the conductor's surface temperature is consistently higher than that of the clamp, and both temperatures increase with rising current. The maximum difference between simulated and experimentally measured conductor surface temperatures was less than 2%, validating the accuracy of the simulation approach.

Keywords
Clamp-conductor system, Electrical current, Thermal stress, Tension force, Overhead power line.

1. Introduction

Overhead power transmission lines are used to transmit electrical energy from power plants to consumers. This transmission is facilitated by bare conductors specifically designed for efficient long-distance energy transfer. The most widely used conductor in the power transmission lines is the Aluminum Conductor Steel-Reinforced (ACSR). ACSR combines the high tensile strength of steel with the superior conductivity and lightweight properties of aluminum, making it ideal for long-span applications. It is engineered to withstand the mechanical stress and harsh environmental conditions typically encountered in power transmission systems, and is therefore widely adopted in many countries [1-6].

The thermal stress on the conductor limits the power transmission capacity of these lines. In other words, the thermal capacity of a transmission line refers to the maximum operating temperature at which it can maintain sufficient clearance and avoid material degradation, such as annealing [7-8]. ACSR conductors are capable of withstanding normal operating temperatures up to 75 °C and emergency operating temperatures up to 127 °C [6].

In an overhead transmission line, conductors are connected to suspension towers using suspension clamps and to tension towers using tension clamps. Tension towers support the mechanical tension of the power lines and are typically installed where lines change direction or terminate. Dead-end tension clamps are used to secure the conductors to these towers. These clamps connect to the tower on one side and grip the conductor firmly on the other. They are crimped onto the conductor using a hydraulic crimping machine, forming an integrated clamp-conductor system [9].

Tension clamps are subjected to significant tensile forces, including the weight of the conductor, additional loads from ice accumulation, and dynamic wind forces [6]. Furthermore, the clamp-conductor system must also withstand thermal stresses resulting from current flow, variations in ambient temperature, lightning strikes, short circuits, and the corona effect, all of which are critical for maintaining reliable power supply [6, 10-12]. A secure and robust connection between the conductor and the clamp is essential during the crimping process. Infrared thermal imaging of weak clamp-conductor connections, as observed in [4], shows that the conductor tends to reach higher temperatures than the clamp. Additionally, the conductor displays symmetrical heat generation in a spiral-like pattern.

Finite element simulation is widely used to analyze electrical machines and high voltage equipment in power systems [13-17]. A simulation study of a clamp-conductor system was conducted in [18] to investigate the tensile strength and failure mode under different crimping conditions. The results showed that the crimping between the steel anchor and the steel core endured the highest tensile force. Also, the tension clamp was able to meet the required tensile strength under standard crimping conditions [18]. Thermal stress analysis on an ACSR conductor under clean and contaminated conditions, as reported in [8], revealed that surface contamination leads to higher temperature variation along the conductor, whereas clean conductors offer better current-carrying performance.

Despite these efforts, limited research has focused on thermal image analysis of clamp-conductor systems in overhead lines.

In this study, a dead-end tension clamp assembly on a Lynx ACSR conductor used in a 63 kV transmission line is simulated. This study aims to analyze the mechanical stresses due to tensile forces and the thermal stresses caused by electrical current. The finite element method (FEM) is employed to simulate these stresses, and the simulation results are validated through current injection tests conducted in a high-voltage laboratory.

Table I. The material properties used in the simulation.

characteristic name	Aluminum	Steel
(J/(kg.K)) Heat capacity at constant pressure	900	475
(W/(m.K)) Thermal conductivity	238	44.5
(S/m)Electrical conductivity	3.774e7	4.032e6
(kg/m^3) Density	2700	7850
(MPa) Young's modulus	70000	203000
Poisson's ratio	0.32	0.3

2. Simulation process

The FEM aims to obtain solutions to complex problems through the use of simplified, discretized models. This approach transforms partial differential equations into systems of ordinary differential equations, enabling the determination of numerical solutions. The problem domain is subdivided into a set of interconnected, smaller subregions known as finite elements. An approximate solution is assumed for each element, and by assembling these elements, the overall equilibrium conditions of the system are established. Optimization of these conditions yields an approximate solution for the quantity of interest. In this study, the geometry of the dead-end clamp and conductor was created in SolidWorks, while the assembly and simulation processes were carried out in COMSOL Multiphysics. SolidWorks, a specialized tool for precise part modeling, offers advanced features for detailed geometry creation. COMSOL, which supports multiple geometric file formats, is a versatile simulation platform capable of modeling and analyzing a wide range of physical phenomena.

2.1. Geometry design

The dead-end tension clamp consists of two primary components: a steel anchor (or steel tube) and an aluminum sheath (or aluminum pipe). This material combination provides the structural strength and durability required for long-term performance under varying environmental conditions. The simulation models of the steel anchor, Lynx conductor, and aluminum pipe, created in SolidWorks, are shown in Figs. 1, 2, and 3, respectively. All geometric dimensions were based on the manufacturer's technical drawings.

The Lynx conductor features a single straight central strand surrounded by three concentric layers containing 6, 12, and 18 strands, respectively. The strand lay direction alternates between clockwise, counterclockwise, and clockwise from the innermost to the outermost layer. In the COMSOL simulation, the seven central strands were assigned steel material properties, while the thirty outer strands were modeled as aluminum.

2.2. Simulation requirements

2.2.1. Assembly

After designing the components in SolidWorks, the parts were imported into COMSOL and assembled under standard conditions in accordance with the manufacturer's assembly drawings. The connection between the conductor and the dead-end clamp is achieved through a three-step crimping process: 1. a portion of the aluminum strands is carefully removed to expose the internal steel strands of the conductor. 2. The exposed steel strands are inserted into the steel tube of the clamp. The steel tube is then crimped onto the conductor steel strands to create a secure mechanical connection. 3. The aluminum tube is crimped in two stages: one part is crimped onto the steel tube, and the other part is crimped onto the aluminum strands of the conductor [9]. This multi-step procedure results in the final assembly, hereafter referred to as the clamp-conductor system, which ensures a reliable and durable connection between the conductor and the dead-end tension clamp. A view of the dead-end clamp assembled on the Lynx conductor is shown in Fig. 4.

2.2.2. Material selection

The studied sample consists of three main parts: the steel anchor, the aluminum pipe, and the Lynx conductor. The steel anchor and the seven central strands of the conductor are made of steel, while the aluminum pipe and thirty outer strands of the conductor are made of aluminum. The material properties used in the simulation are summarized in Table I. The heat capacity of the material refers to the amount of heat (in joules) that must be applied to one kilogram of the material to raise its temperature by one kelvin. Thermal conductivity describes the material's ability to transfer heat. Yield strength refers to the maximum stress that can be applied to a material before it begins to undergo permanent deformation, i.e., the limit up to which it retains its elastic properties. Furthermore, tensile strength refers to the maximum tensile force that a material can withstand per unit area without breaking.

2.2.3. Boundary conditions

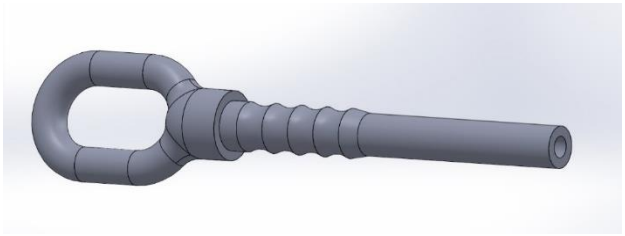

Fig. 1. Steel anchor simulation

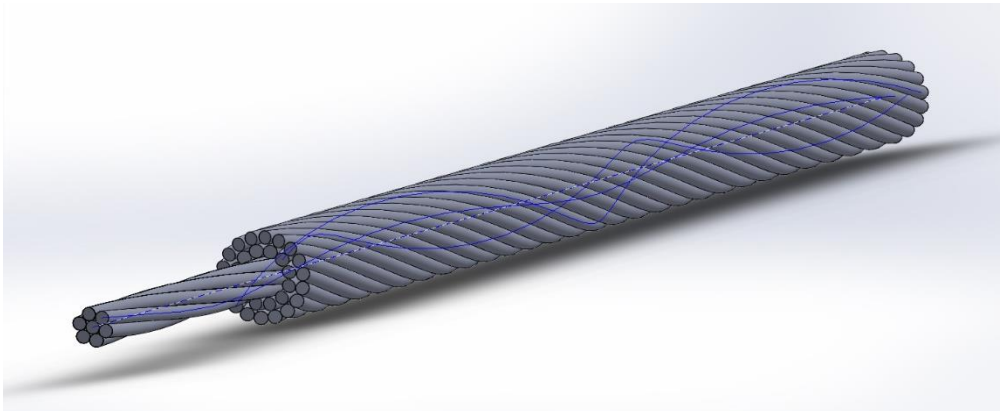

(a)

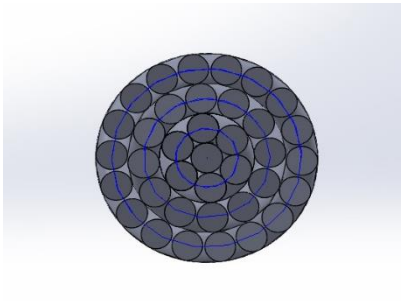

(b)

Fig. 2. Lynx conductor simulation, a) front view, b) cross-sectional view.

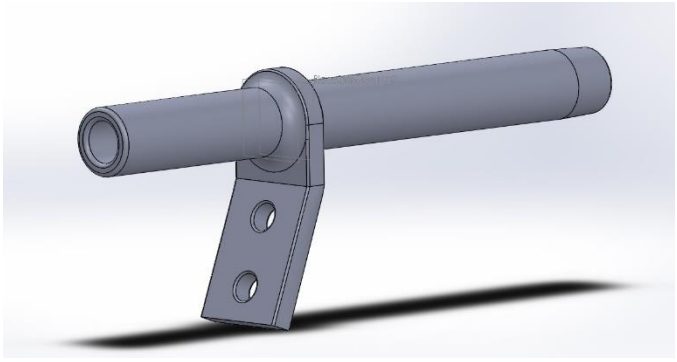

Fig. 3. A view of aluminum pipe simulation.

This study consists of two parts: mechanical simulation and thermal simulation. The mechanical simulation aims to determine the stress distribution by numerically solving the stress-strain equation, which predicts the material deformation of a substance with linear elastic properties. The stress-strain equation is:

$$\nabla . S + F_V = 0 \quad (1)$$

where S denotes stress, and F_V represents strain. Two boundary conditions are needed to solve this equation. The first boundary condition is a fixed constraint, where the end section of the steel anchor is considered fixed. The second boundary condition is the force applied to the

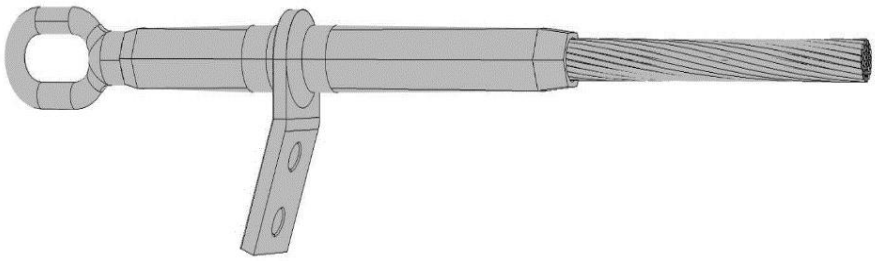

Fig. 4. A view of dead-end clamp assembled on the lynx conductor.

conductor, which acts on the cross-sectional area at the conductor's end. The fixed and the force-applied bounds are shown in Fig. 5.

In this study, the force applied to the end of the conductor varies with time and is increased uniformly at a rate of 1 kN/s. Once the Specified Minimum Failure Load (SMFL) of 77.3 kN is reached, it is maintained constant for a duration of one minute. The SMFL value corresponds to 95% of the Ultimate Tensile Strength (UTS) of the Lynx conductor. After reaching the SMFL, the applied force is further increased and then terminated at 85 kN.

The second part of this study focuses on simulating the thermal stress experienced by the sample under electric current injection. The temperature distribution within the sample during current flow is determined by solving the general heat transfer differential equation, as given below:

$$\rho.C_p.u.\nabla T = \nabla.(k\nabla T) + Q_e \quad (2)$$

Where C_p is the specific heat capacity, ρ is the density of the material, k is the thermal conductivity, T is the temperature, ∇ is the gradient operator, and u is the fluid velocity. Due to the absence of fluid movement, this value is zero. Q_e represents the heat generated or consumed in the system. The heat produced in the system is due to the electrical current, which is calculated using the electrical current physics. When current flows through a material, it generates heat due to the resistance of the material (Joule heating). Joule heating, also known as resistive or ohmic heating, is the process where electrical energy is converted into thermal energy as an electric current flow through a conductor. When an electric current passes through a conductor, electrons move through the material. These moving electrons collide with the atoms of the conductor. These collisions transfer energy from the electrons to the atoms, increasing the kinetic energy of the atoms and thus raising the temperature of the material. This heat generation term is then incorporated into the heat equation, and solving it determines how the temperature distributes throughout the sample.

The heat generated in the conductor is transferred to the environment through the surrounding air. Finally, the general heat transfer equation in the studied system becomes:

$$\nabla.(k\nabla T) + Q_e = 0 \quad (3)$$

The solution of equation (3) yields the temperature distribution across the clamp-conductor system, with the ambient air temperature in the simulation set to 20 °C.

2.2.4. Meshing

Meshing plays a critical role in ensuring the accuracy of finite element modeling results. Higher mesh accuracy is applied in regions subjected to deformation and at sharp corners, where smaller elements and higher node densities are used. The generated mesh consists of 1,102,506 elements, including both tetrahedral and triangular types. The smallest element dimension is 0.03 mm, while the average element size is 0.6 mm. The views of the studied sample are shown in Fig. 6.

3. Simulation results

The mechanical and thermal stresses on the studied sample have been investigated and analyzed. Von Mises stress distribution under a 77.3 kN force is shown in Fig. 7.

The Von Mises criterion is a formula used in materials science and engineering to predict the yielding of ductile

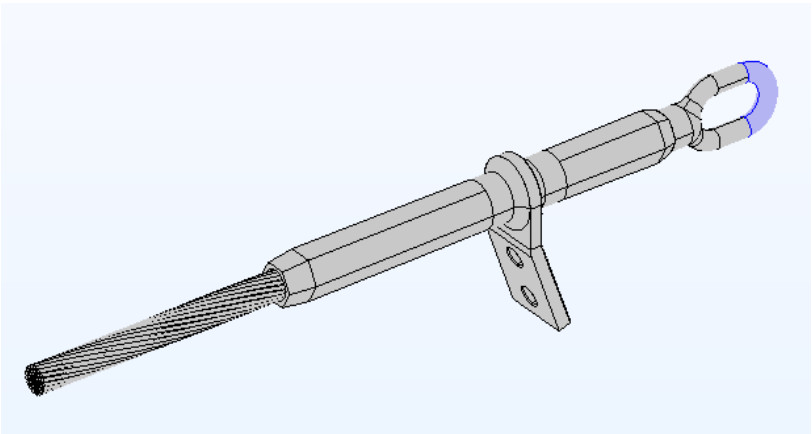

Fig. 5. The fixed bound (purple color) and force-applied bound (black color) in the mechanical tension simulation.

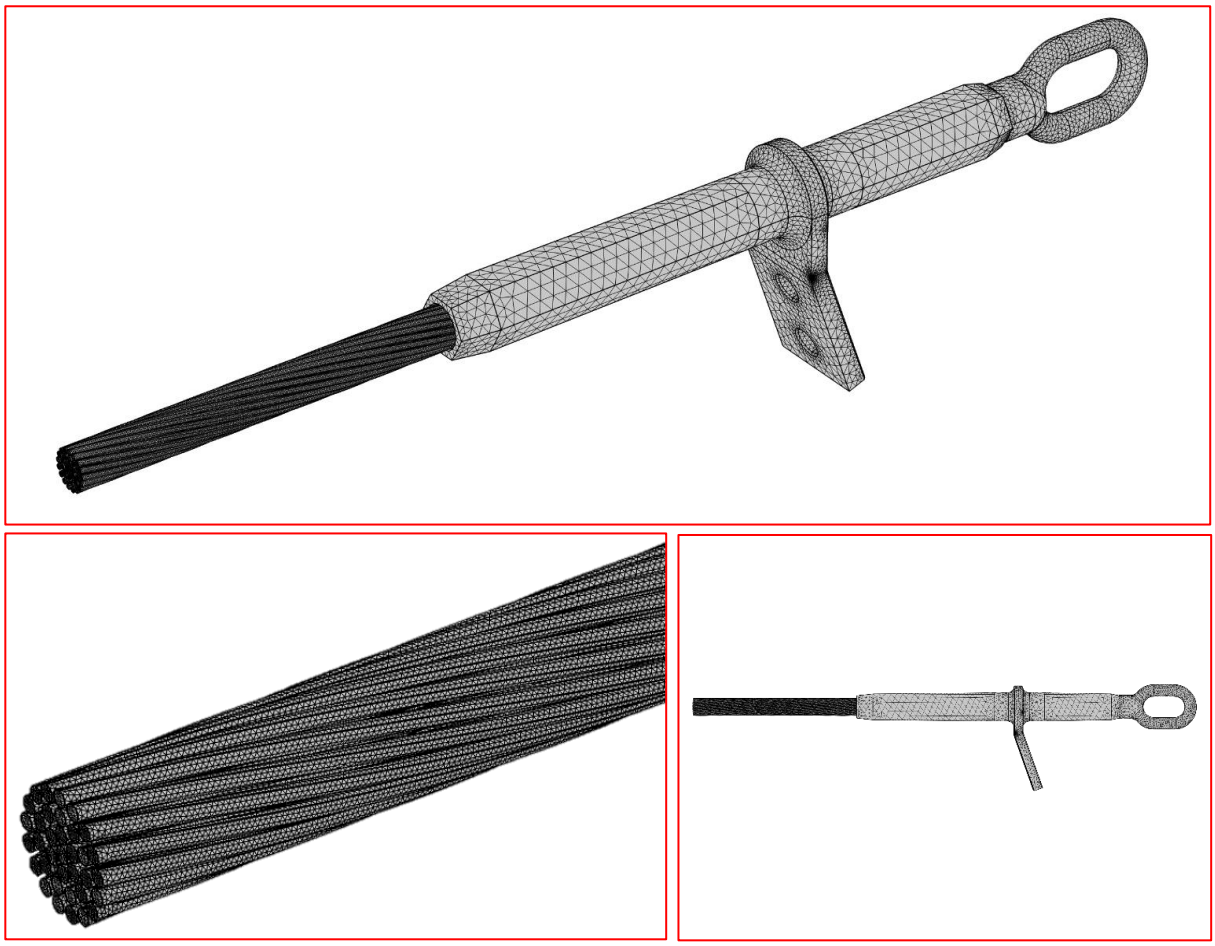

Fig. 6. Meshing images of the studied clamp-conductor system.

Fig. 7. Von Mises stress distribution under 77.3 kN .

materials under complex loading conditions. It's a yield criterion, meaning it tells us when a material will start to permanently deform (yield), not necessarily break. The tensile strength of a conductor typically refers to its UTS, which is the maximum stress it can withstand while being stretched before breaking. The von Mises criterion is not about ultimate strength but about yield strength, which is the stress level at which plastic (permanent) deformation begins.

For better visualization of the results, the aluminum pipe is depicted as semi-transparent. As observed, the highest mechanical stress is concentrated in the central (core) part

of the conductor, which bears the majority of the applied force. Additionally, significant stress is experienced at the end of the steel anchor. The results also indicate that the jumper terminal endures moderate mechanical stress.

Furthermore, the displacement of the clamp-conductor system under tensile force is illustrated in Fig. 8. As shown, the greatest displacement occurs in the steel core of the conductor. However, the maximum displacement observed under the application of a 77.3 kN force is approximately 190 nm.

To accurately simulate the thermal behavior of the studied sample, it is essential to establish the current flow path and quantify the electric current levels. The lower surface of the jumper terminal serves as the starting point, while the cross-sectional area at the end of the conductor is designated as the endpoint. With these surfaces identified, the electric current flows from the start to the end of the path. Two current levels, 470 Amps (normal load) and 600 Amps (overload), are applied to the sample, based on actual operational data from the Lynx conductor used in Iran's 63 kV overhead power lines [9].

The temperature distribution on the surface of the sample at 470 Amps and 600 Amps is illustrated in Figs. 9 and 10, respectively. To improve the visualization of the conductor's temperature, the aluminum pipe is depicted as semi-transparent. The temperature variation pattern on the conductor surface and clamp remains consistent under both normal load and overload conditions; however, the surface temperature of the conductor and clamp is higher under overload compared to normal load. Additionally, simulation results indicate that the clamp surface temperature is lower than that of the conductor, a finding corroborated through thermographic imaging during the laboratory current injection test [9]. According to the simulation findings, the maximum surface temperatures of the conductor under normal load and overload conditions are 51°C and 77°C, respectively. There is only a low discrepancy between these findings and the thermal imaging results for Sample 1 obtained in [9].

4. Thermal stress test

The electric current injection test is a key procedure for assessing the thermal performance of electrical fittings and conductors. This section details the laboratory setup, presents the temperature distribution of the studied sample, and discusses the thermovision imaging analysis.

Laboratory requirements

The electric current injection test was performed on the studied sample at the high-voltage laboratory of Niroo Research Institute (NRI). Niroo Research Institute plays a leading role in developing new technologies for Iran's electric power industry. The electric current injection test was conducted using a transformer with a voltage ratio of 220/5 volts and a rated apparent power of 50 kVA [9]. Fig. 11 shows the output terminals of the transformer. To adjust the transformer's output current, the voltage regulator control panel, shown in Fig. 12, is used. Thermal imaging of the studied sample was performed using the HotFind-S thermovision camera, manufactured by SATIR Europe, based in Ireland. The technical specifications of this camera are provided in [9]. The dead-end clamp is assembled on the conductor according to the standard method recommended by IEC-61284 [19].

Fig. 8. The displacement of the clamp-conductor system under the 77.3 kN .

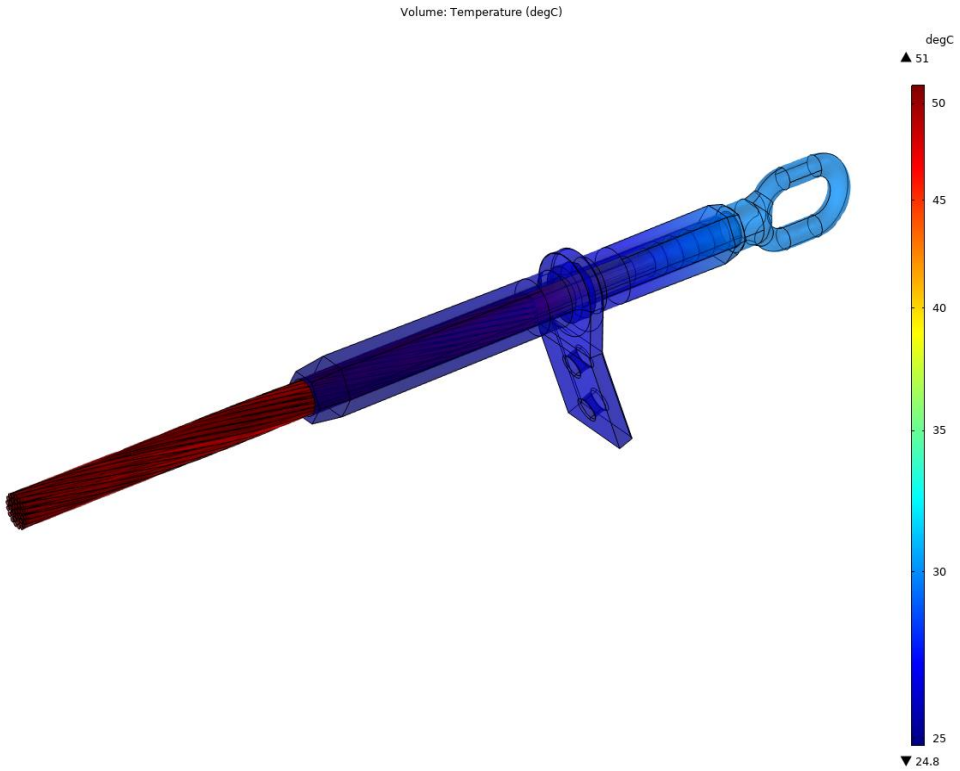

Fig. 9. Temperature distribution (ºC) on the clamp-conductor system under 470 A.

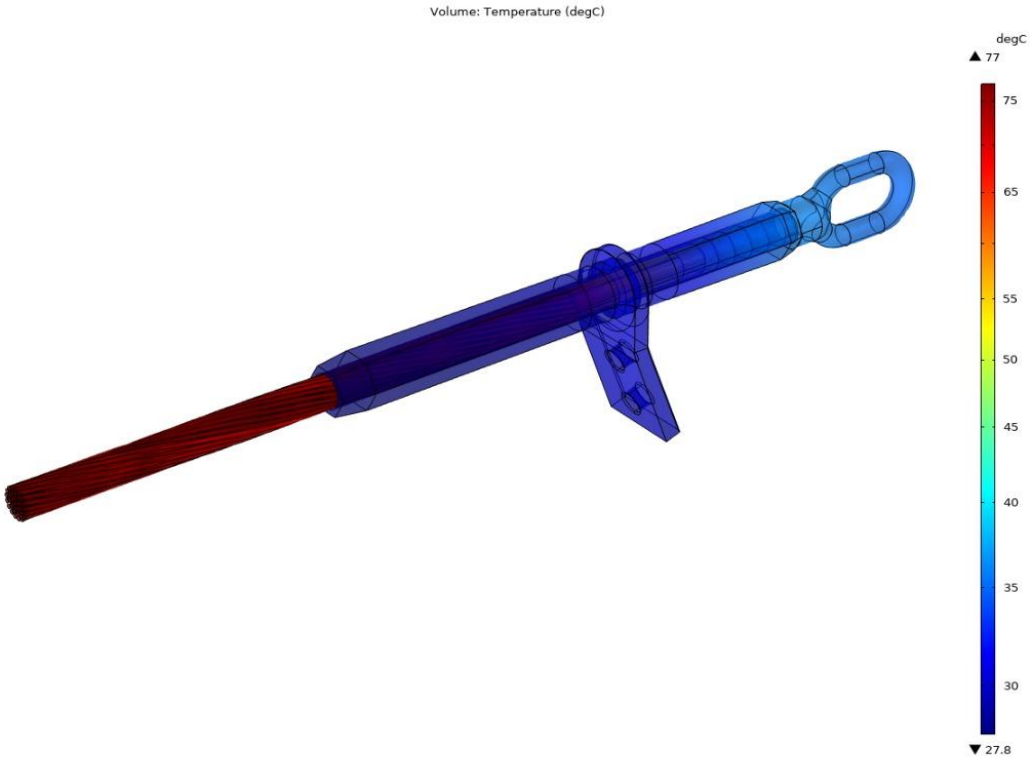

Fig. 10. Temperature distribution (ºC) on the clamp-conductor system under 600 A.

A view of the studied sample, installed on the transformer terminals and ready for the electric current injection test, is shown in Fig. 13.

Test results

The current injection test was conducted at two current levels: one within the normal load range (470 amps) and the other at an overload current level (600 amps), which corresponds to the current-carrying capacity of the Lynx conductor used in 63 kV transmission lines. After applying the electric current and allowing the sample's

Fig. 11. Output terminals of single-phase transformer used for current injection test.

Fig. 12. Voltage regulator control panel used for current injection test.

Fig. 13. A view of studied sample ready for current injection test.

surface temperature to stabilize, thermal imaging was performed using a thermovision camera. The results of the thermal imaging of the sample are presented in Table II. Table II also provides the following details: the average laboratory environment temperature, the maximum temperature of the dead-end clamp, as well as the conductor's maximum temperature under both normal load and overload conditions. An image captured from the studied sample using a thermovision camera is presented in Fig. 14.

The results indicated no abnormalities in the thermographic image of the studied sample. The surface temperature of the dead-end clamp was lower than that of the conductor. Moreover, increasing the electric current resulted in a corresponding rise in the surface temperatures of both the conductor and the clamp, with the conductor exhibiting a greater temperature increase than the clamp.

The results show a high level of agreement between the surface temperatures of the conductor and clamp obtained from both the simulation and the current injection test. Under effective current values of 470 A and 600 A, the conductor's maximum temperatures recorded during the current injection test were approximately 52°C and 76°C, respectively, while the corresponding temperatures from the finite element simulation were 51°C and 77°C. This indicates a maximum deviation of less than 2% between the simulation and experimental results, demonstrating the accuracy of the simulation model.

5. Conclusions

In this study, mechanical and thermal stress simulations of a clamp-conductor system were conducted using the finite element method. The results indicate that the steel core of the conductor experiences the highest mechanical stress. Additionally, the thermal distribution pattern within the clamp-conductor system remains consistent under both normal and overload conditions. The conductor experiences the highest thermal stress, while the surface temperature of the tension clamp is

Table II. The thermal imaging results of the studied sample under the electric current injection test.

effective current value (A)	ambient temperature (°C)	Conductor's maximum temperature (°C)	Dead-end clamp's maximum temperature (°C)
470	19.4	52.3	30.7
600	19.8	75.8	36.5

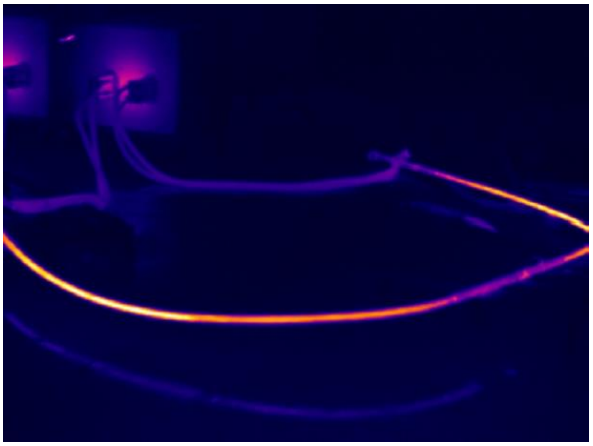

Fig. 14. The thermal image of studied sample by thermovision camera under 470 A.

lower than that of the conductor. The maximum surface temperatures of the conductor under normal and overload conditions are about 51°C and 77°C, respectively, which is below the thermal limit of the Lynx conductor. Subsequently, a current injection test was conducted in a high-voltage laboratory on the same sample. The conductor's maximum temperature under an effective current value of 470 A and 600 A is approximately 52°C and 76°C, respectively. The maximum deviation between the simulation and experimental results was found to be less than 2%, confirming the accuracy of the simulation model. The results obtained in this study can be used to evaluate the thermal stress of tension clamps and fittings by a thermovision camera under the normal and overload conditions on a 63 kV overhead power lines.

6. References

[1] S. Lalonde, R. Guilbault, S. Langlois, "Numerical Analysis of ACSR Conductor–Clamp Systems Undergoing Wind-Induced Cyclic Loads*", IEEE Transactions on Power Delivery,* vol. 33, no. 4, pp. 1518-1526, 2018.

[2] J. Liu, B. Yan, G. Huang, et al., "Study on mechanical characteristics of conductors with three-dimensional finite-element models", *Royal Society Open Science,* vol. 7, no. 5, (200309), 2020.

[3] J. Said, S. Fouvry, G. Cailletaud, et al., "A global–local approach to predict the fretting-fatigue failure of clamped aluminum powerline conductors: From mono-contact crossed wires to full conductor vibrational tests", *Engineering Failure Analysis*, vol. 146, (107073), 2023.

[4] Y. Jin, M. Quan, S. Yan, et al., "Analysis of overhead transmission lines fusing failure due to poor contact between conductors and clamps", *Engineering Failure Analysis*, vol. 118, (104858), 2020.

[5] B. Burks, D.L. Armentrout, M. Kumosa, "Failure prediction analysis of an ACCC conductor subjected to thermal and mechanical stresses", *IEEE Transactions on Dielectrics and Electrical Insulation,* vol. 17, no. 2, pp. 588-596, 2010.

[6] N.M. Zainuddin, M.S. Abd Rahman, M.Z.A. Ab Kadir, et al., "Review of Thermal Stress and Condition Monitoring Technologies for Overhead Transmission Lines: Issues and Challenges", *IEEE Access,* vol. 8, pp. 120053-120081, 2020.

[7] S. Karimi, P. Musilek, A.M. Knight, "Dynamic thermal rating of transmission lines: A review", *Renewable and Sustainable Energy Reviews*, vol. 91, pp. 600-612, 2018.

[8] L. Zhao, R. Wang, P. Dai, et al., "Influence of contamination on the axial temperature profile of ACSR conductors", *Electrical Engineering*, vol. 105, pp. 733-743, 2023.

[9] J. Dadashizadeh Samakosh, F. Enayati, "Operation Recommendations for Tension Joints and Clamps on a 63 kV Overhead Transmission Line Conductor Based on Experimental Tests", *Electric Power Components and Systems,* vol. 51, no. 7, pp. 639-655, 2023.

[10] X. Zhang, Z. Ying, Y. Chen, X. Chen, "A thermal model for calculating axial temperature distribution of overhead conductor under laboratory conditions", *Electric Power Systems Research*, vol. 166, pp. 223-231, 2019.

[11] W. Yang, Z. Zheng, W. Huang, et al., "Thermal analysis for multi-conductor bundle in high voltage overhead transmission lines under the effect of strong

wind", *Electric Power Systems Research*, vol. 231, (110308), 2024.
[12] L. Beňa, V. Gáll, M. Kanálik, et al., "Calculation of the overhead transmission line conductor temperature in real operating conditions", *Electrical Engineering,* vol. 103, pp. 769-780, 2021.
[13] R. Rostaminia, M. Sanei, A. Akbari, "The Effect of Power Electronic Device Pulses on Partial Discharge in Electrical Machine Insulation Using Finite Element Modeling", *Journal of Electrical Engineering, University of Tabriz*, Vol. 45, Issue 1, pp. 21-21.
[14] A. Darabi, A. Behniafar, H. Tahanian, H. Yousefi, "Modeling the Steady-State Performance of a Cylindrical Inverted Hysteresis Motor Using the Finite Element Method", *Journal of Electrical Engineering, University of Tabriz*, Vol. 47, No. 3, pp. 1001-1012, 2017.
[15] J. Dadashizadeh Samakoosh, M. Mirzaei, "Simulation and analysis of the effect of uniform and non-uniform (longitudinal and cross-sectional) contamination on the potential and electric field distribution of polymer insulators using the finite element method", *Journal of Modeling in Engineering*, Vol. 17, Issue 56, pp. 1-12, 2019.
[16] S. M. Seyyedbarzegar, and M. Mirzaie, "Electro-thermal modeling of surge arrester based on adaptive power loss estimation using finite element method." *International Transactions on Electrical Energy Systems*, vol. 26, no. 6, pp. 1303-1317, 2016.
[17] S. M. Seyyedbarzegar, and M. Mirzaie, "Heat transfer analysis of metal oxide surge arrester under power frequency applied voltage", *Energy*, vol. 93, pp. 141-153, 2015.
[18] Z. Ye, K. Pang, Y. Du, et al., "Simulation Analysis of the Tensile Mechanical Properties of a Hydraulic Strain Clamp-Conductor System", *Advances in Materials Science and Engineering*, (4591812), 2020.
[19] *IEC-61284 Standard*, "Overhead lines: requirements and tests for fittings", 1997.